Study of the industrial potential of Markforged X7 3D printer

Daouda Nikiema, Alain Sergent, Pascale Balland

Mechanics & Industry **25**, 4 (2024)

https://doi.org/10.1051/meca/2024003

Mechanics & Industry

Available online at:
www.mechanics-industry.org

REGULAR ARTICLE

OPEN ACCESS

Study of the industrial potential of Markforged X7 3D printer

Daouda Nikiema*, Alain Sergent, and Pascale Balland

Université Savoie Mont Blanc, SYMME, Annecy, 74000 France

Received: 16 June 2023 / Accepted: 18 January 2024

Abstract. Additive Manufacturing (AM) using Fused Deposition Modelling (FDM) is a 3D printing technique that can produce parts with complex shapes. Multiple types of 3D printers are available in the market, so it is essential to understand their potential to manufacture parts that meet industry standards. This study aims to evaluate the industrial potential of the Markforged X7 printer by assessing its performance based on the QS9000 quality standard. The quality indices, including the Cp index and the Cpk index, were determined for different dimensions, and admissible tolerances were identified for geometrical defects. The study shows that the quality indices, especially the Cp index, are within an acceptable range of 1.6 to 2 for the class 12 tolerance interval (IT12). The geometrical defects are predominantly categorized as fine according to the ISO 2768 standard, with deviations in geometrical features ranging from 0.06 to 0.08 mm. Additionally, the study investigated the impact of moisture and glass fiber reinforcement on the geometrical features. The analysis indicated that moisture increases deviations in the features. However, adding reinforcing fibers does not improve deviations but stabilizes them under the effect of moisture.

Keywords: 3D printing / dimensions and geometry deviations / quality index / glass fiber / moisture effect

1 Introduction

The FDM process has undergone significant advancements in recent years, transforming from a method for prototyping into a means for producing functional parts in a variety of industries, including medical, aerospace, rail, and automotive. One of its major advantages is the ability to manufacture geometrically complex parts of acceptable quality [1]. For instance, a reduced-size Eiffel Tower with intricate details was successfully printed using the FDM process by Surya Teja et al. [2]. During the COVID-19 pandemic, FDM was utilized to print medical devices [3]. To be suitable for the production of small or medium series in industrial applications, FDM must meet certain standards and functional dimensioning plans. Kandananond et al. [4] employed artificial intelligence to predict the surface roughness of FDM printed parts based on input data including bed temperature, printing speed, and layer thickness. Lieneke et al. [5] experimentally determined dimensional tolerances for FDM, finding them to be comparable in performance to other manufacturing processes such as sintering, drilling, cutting, and milling. In another study, Maurya et al. [6] investigated optimal process parameters and IT classes by varying layer thickness, orientation, and raster angle. Minetola et al. [7] compared the dimensional accuracy of three FDM printers according to ISO IT classes, concluding that a smaller layer thickness yields better accuracy. Galantucci et al. [8] similarly compared the dimensional accuracy of a cubic part printed with an industrial 3D printer and an open-source printer, finding the former to be more accurate. Maurya et al. [9] examined the influence of infill pattern and density on the dimensional accuracy and printing time of a cube part printed with an Ultimaker 2+ FDM machine. Nidagundi et al. [10] explored the impact of layer thickness, orientation, and raster angle on dimensional accuracy and surface roughness, finding that layer thickness had the greatest influence on both, followed by orientation and raster angle.

Understanding the quality of a manufacturing process is crucial before using it to produce parts. According to Wu et al. [11], capability indices (Cp, Cpk, Cpm, and Cpmk) are an effective and standard tools for assessing quality. However, Anis et al. [12] found that these indices are not always consistent. Mahshid et al. [13] have mainly considered the intrinsic process capability Cp, along with measuring uncertainty and tolerance limits, to determine conformity and non-conformity to quality requirements for part characteristics. Günay et al. [14] combined process capability indices and design of experiment (DOE) to find optimal parameters for achieving high accuracy in dimensions. They concluded that FDM can be comparable

* e-mail: daouda.nikiema@univ-smb.fr; daoudanikiema94@gmail.com.

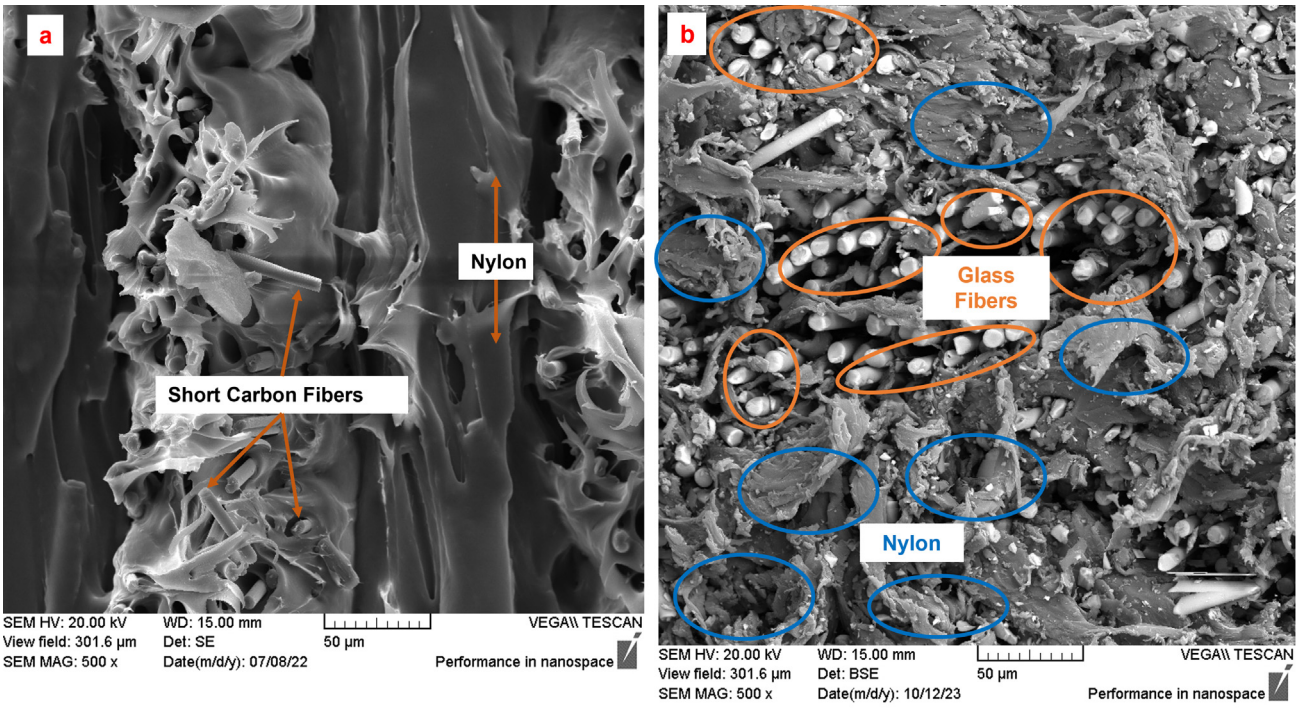

Fig. 1. Materials used in this study: (a) Onyx and (b) Glass fibers.

to certain traditional manufacturing processes. Ranjan [15] also used capability indices to evaluate the performance of twin-screw extruder processes in producing feedstock filament for 3D printers. Wooluru et al. [16] demonstrated the importance of capability indices in controlling and ensuring product quality to meet customer requirements, through a case study in the automotive industry.

One of the main drawbacks of 3D printed materials is their tendency to absorb humidity, causing dimensional and geometric instability. Aclan et al. [17] confirmed this in their study. Clavería et al. [18] explored the impact of environmental conditions on dimensional stability for injected parts in Polyamide 6 (PA6) and Polyamide 66 (PA66), finding an average dimension variation of 12% for PA6 and 3% for PA66.

Although many studies have been conducted on research and office printers, few have been performed on industrial printers. Therefore, the aim of this study is to assess the potential of Markforged X7 industrial printer using standard indices (Cp and Cpk) and investigate the effects of moisture and the addition of fibers. These investigations are important to help users understand the capabilities of this printer. The study was conducted in several stages, starting with an introduction of the materials and methods, followed by the presentation of the results and discussion, and concluding with proposed perspectives.

2 Material and method

2.1 Printer, material and studied part

The 3D printer used in this study is the Markforged X7 industrial series, a commercial printer with a printable volume of 330 mm × 270 mm × 200 mm, which is relatively large compared to other printers. The printer can produce industrial parts of various sizes based on the quality requirements of the part and can print using only plastics material or plastics reinforced with long fibers [19]. The printer has several print variables that can be accessed through its cloud slicing software, Eiger, such as layer thickness (ranging from 0.05 mm to 0.25 mm), type of patterns (triangular, rectangular, hexagonal, gyroid, and solid), number of walls, type of fibers (glass, carbon, and Kevlar), orientation angle of the fibers, and fibers placement mode (concentric, isotropic) [20].

For this study, the Onyx material was used to print the parts. Onyx is a black filament with a diameter of 1.75 mm produced by Markforged. It is made of nylon (Polyamide 6) filled with approximately 10 to 20% of micro carbon fibers (Fig. 1a), which provides satisfactory precision and surface finishes. According to the manufacturer, it also has good mechanical properties and chemical resistance. Hetrick et al. [21] found that the length of carbon fibers in Onyx varies from 7.035 to 44.58 µm, and the fibers are mainly oriented in the deposition direction of the material. In the present work, continuous glass fibers consisting of a mixture of nylon and glass fibers (approximately 33% of continuous glass fibers, 59% of nylon, and 8% of void in volume) were also used to reinforce Onyx parts. (Fig. 1b) shows a scanning electron microscopic image of the glass fiber filament.

To conduct the study, a part model was designed in SolidWorks software and printed in Onyx material alone and Onyx with glass fiber. The part model included a set of geometric and dimensional characteristics typically found on industrial parts, such as a hole, an inclined plane, parallel planes, and perpendicular planes. A batch of 30 pieces was printed simultaneously in order to have a

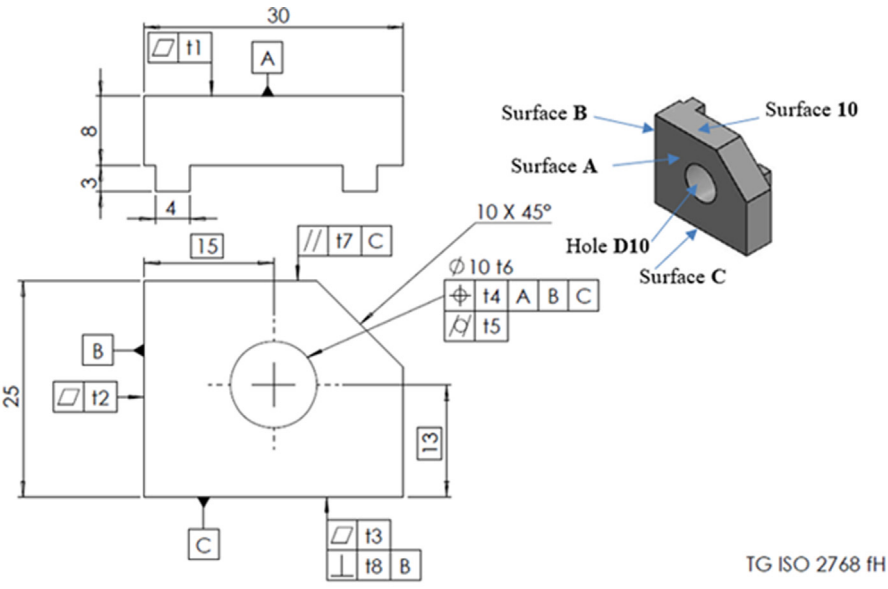

Fig. 2. Views of the workpiece, surfaces and features nomenclature.

Table 1. Printing parameters.

Parameters	Specifications
Pattern and density	Triangular - 37%
Layer thickness – wall width	0.1 mm – 0.4 mm
Walls (contours) count	2
Roof and floor layers	4
Printing time for one part	56 min

number of data representative enough to perform a consistent statistical analysis. Figure 2 displays the part model and all the measured features, dimensions, and nomenclatures used in this study. The printing parameters are summarized in Table 1 and represent the default parameters provided by the slicer of the printer.

2.2 Moisture and fibers reinforcing influence

In order to study the impact of moisture absorption on the geometrical features, the printed parts were exposed to an ambient environment with a relative humidity of 32% at 20 °C. After a period of three months, the geometrical features of the parts were measured and analyzed. It is important to note that Onyx material, which was used to print the parts, is sensitive to humidity due to its composition of Polyamide 6 (PA6) material. This sensitivity to humidity has been previously confirmed in literature. In a previous study, it was shown that Onyx can absorb up to 1.8% humidity in three months of exposure [22]. The impact of humidity on the Onyx filament has not been studied or taken into account. However, the filament is protected in a 'dry box' to prevent aging under the influence of humidity. The study only focused on the impact of humidity on the final printed parts.

The study also analyzed the effect of reinforcement fibers on stabilizing the deviations of the geometric features. To achieve this, the parts were reinforced with glass fibers at different angles (0°, 90°, and +/− 45°), as shown in Figure 3.

2.3 Measurement instruments

A Mitutoyo coordinate measuring machine (CMM) was used for the measurements, as shown in Figure 4, similar to previous studies in the literature like [23]. The manufacturer's indicated resolution of the CMM is $(1.9 + 0.3L/100)$ µm, where L is the maximum length of the measured part, and in our case, L = 30 mm, resulting in a resolution of 1.99 µm. The measurement dispersion was evaluated in a previous study and is summarized in Table 2. Other measurements, such as direct dimensions, were taken using a digital caliper with a resolution of 0.01 mm, which has also been used in previous studies [14]. The results obtained from the measurements were analyzed using a statistical analysis method and the ELLISTAT statistical software developed at the SYMME laboratory of the University of Savoie Mont Blanc [24]. This method of statistical analysis, combined with the use of statistical software, was previously utilized by Khodygan et al. [25] and by Rathor et al. [23] in their respective works.

2.4 Method of analysis

When evaluating the quality of a machine, the production process is evaluated on the basis of their capability indices. The most frequently utilized indices are Cp and Cpk, which are calculated using equations (1) and (2), respectively.

$$\mathrm{Cp} = \frac{\mathrm{USL} - \mathrm{LSL}}{6\sigma} \text{ or } \mathrm{Cp} = \frac{\mathrm{IT}}{6\sigma}. \quad (1)$$

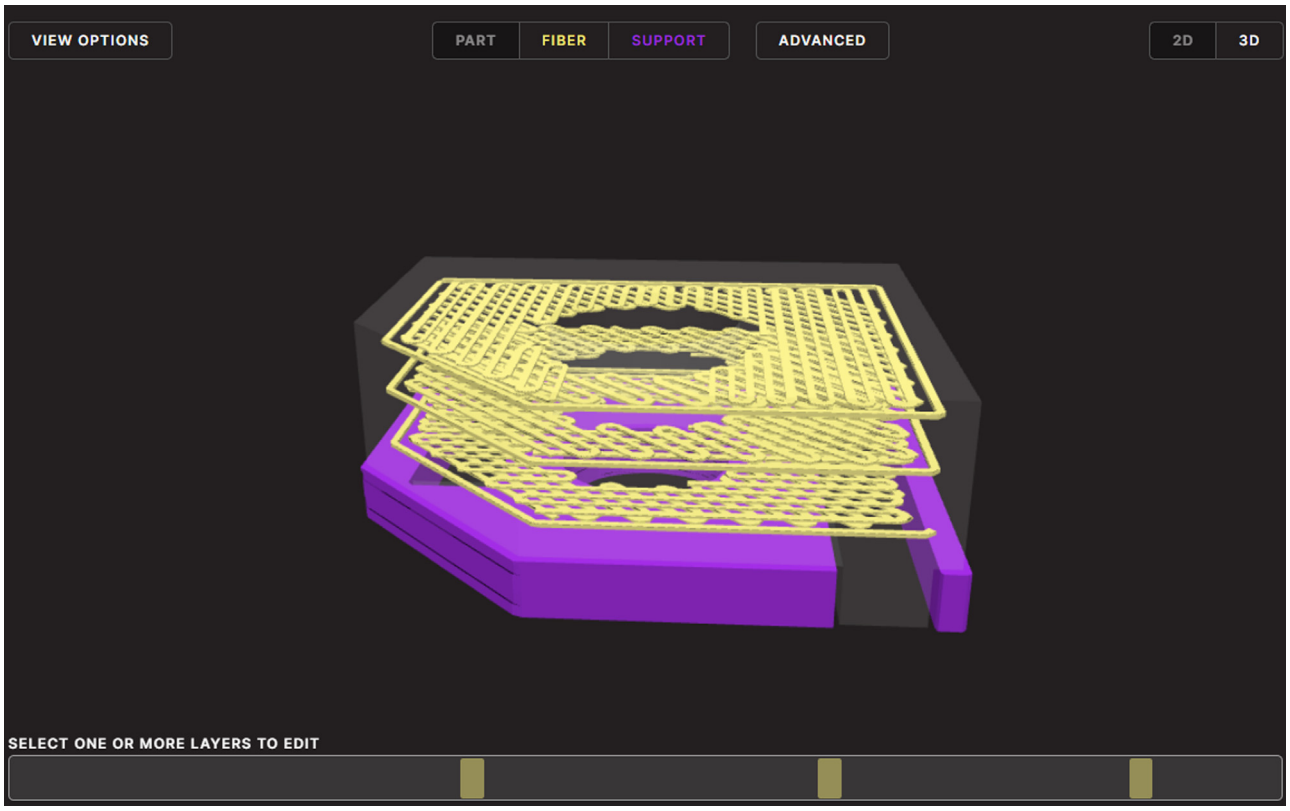

Fig. 3. Reinforced part.

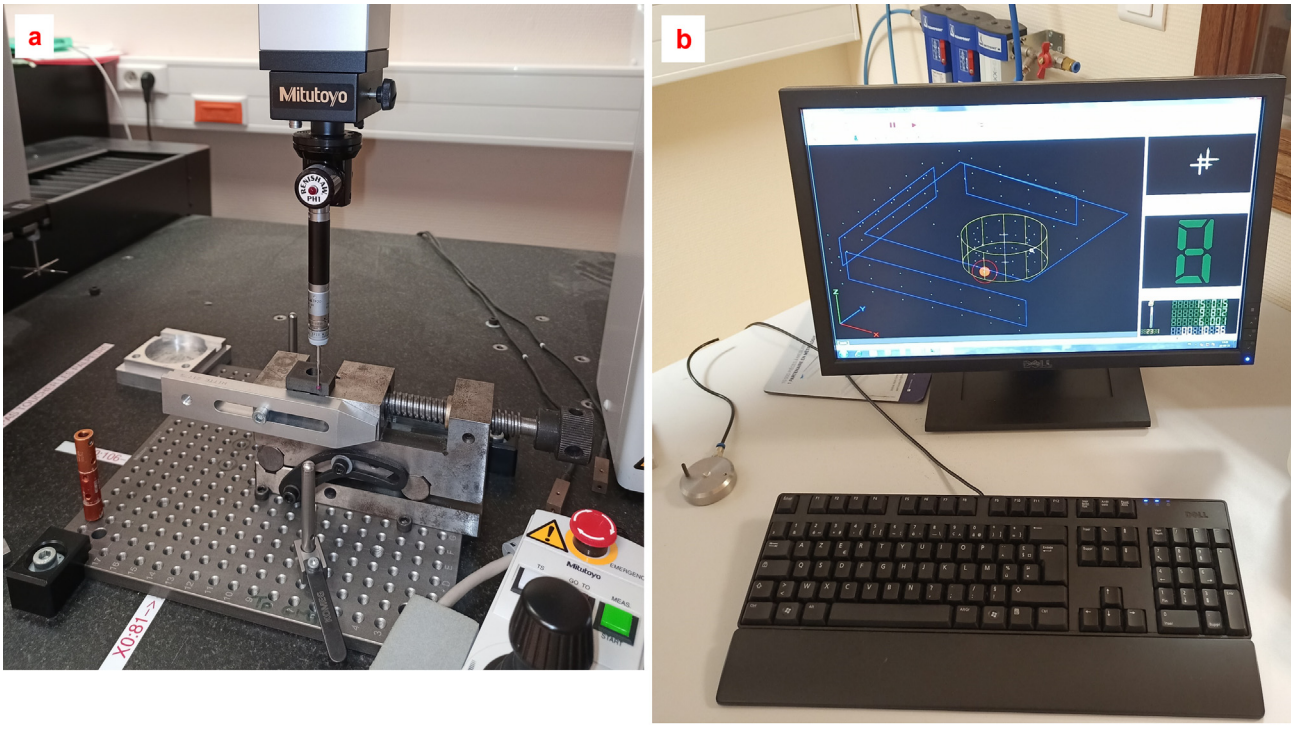

Fig. 4. CMM measurement and data collection. a: Mitutoyo Chrysta 544 machine and b: Mcosmos software.

Table 2. Measurement dispersion of the Mitutoyo CMM according to X, Y and Z directions; D is a hole's diameter dispersion.

Parameters	X	Y	Z	D
Measurement dispersion (mm)	0.002	0.002	0.004	0.005

Table 3. IT classes and summary of calculated indices for Onyx parts. Units of dimensions are mm.

IT	Dimension C25				Dimension C30				Diameter D10			
	IT (mm)	Cp	Cpk	%NC	IT (mm)	Cp	Cpk	%NC	IT (mm)	Cp	Cpk	%NC
IT7	0.027	0.21	–2.51	**94.67**	0.027	0.25	–1.31	**99.99**	0.015	0.21	–2.46	**100**
IT8	0.033	0.25	–0.50	**93.02**	0.033	0.31	–1.65	**99.99**	0.022	0.31	–2.36	**100**
IT9	0.052	0.40	–0.35	**85.20**	0.052	0.48	–1.07	**99.94**	0.036	0.5	–2.17	**100**
IT10	0.084	0.64	–0.11	**62.48**	0.084	0.78	–0.78	**99.02**	0.058	0.81	–1.86	**100**
IT11	0.130	0.99	0.24	**23.35**	0.130	1.20	–0.35	**85.44**	0.090	1.25	–1.42	**99.99**
IT12	0.210	1.60	0.85	**0.54**	0.210	1.95	0.39	**12.17**	0.150	2.08	–0.58	**95.99**
Average value ($\overline{X}$)			25.049				30.084				9.904	
Average deviation			+ 0.049				+ 0.084				–0.096	
Dispersion (6σ)			0.132				0.108				0.072	
Maximum value			25.09				30.11				9.924	
Minimum value			25.01				30.05				9.878	
Target			25				30				10	

%NC: represents the percentage of non-conforming parts. For example, for dimension **C25** with IT12, 0.54% of non-conformity parts is observed if this tolerance interval.

Cp is an inherent measure of a process's capability. *USL*, *LSL*, IT, and σ represent the upper specification limit (maximum permissible value), lower specification limit (minimum permissible value), tolerance interval, and standard deviation, respectively. Cp indicates that the production variability is consistent with the tolerance interval. Typically, for a process to be considered capable, the ratio between the tolerance interval and the variability must be greater than 1.33, [16,26].

$$\mathrm{Cpk} = \min\left\{\frac{\mathrm{USL} - \overline{\mathrm{X}}}{3\sigma}, \frac{\overline{\mathrm{X}} - \mathrm{LSL}}{3\sigma}\right\}, \tag{2}$$

$\overline{\mathrm{X}}$: being the average value of the measurements. The Cpk index indicates whether the process is centered or not in the band 6σ (dispersion) on the target value.

Interpretations of the quality indices:

- $\mathrm{Cp} > 1.33$ indicates that the process is inherently capable.
- $1 < \mathrm{Cp} < 1.33$ indicates that the process requires monitoring [23].
- $\mathrm{Cp} < 1.33$ indicates that the process cannot produce a large number of parts within the specified tolerances [14].
- $\mathrm{Cpk} < \mathrm{Cp}$ indicates that the process is off-centered.

The calculation of capability indices involves determining the upper specification limit (USL) and lower specification limit (LSL) based on the allowed tolerance interval (IT) for the dimensions. The ISO 286-1 standard [27], which deals with geometric product specifications, provides tolerance classes for linear dimensions based on their sizes. In this study, IT classes ranging from 7 to 12 were used based on the capability study conducted by Günay et al. [14]. For geometric features such as flatness, perpendicularity, parallelism, and cylindricity deviations, the maximum tolerance allowed by the printer is determined, and the value of Cp is fixed at 1.33, with the tolerance obtained using relation 3.

$$\mathrm{IT} = \mathrm{Cp} * 6\sigma. \tag{3}$$

3 Results and discussion

3.1 Results for linear dimensions

The ISO 286-1 standard defines a direct or linear dimension as the distance between two opposing parallel surfaces. Based on this definition and the CAD for this study, the dimensions selected were **C25** and **C30**, which were measured using a digital caliper, as was done in the study by Gradl et al. [28]. The diameter of the hole (**D10**) was also considered as a linear dimension, as assumed by Rathor et al. [23]. This assumption is justified because holes made using FDM typically receive inserts, usually metallic ones. The diameter of the hole was measured using the CMM. The IT class used for each dimension studied is summarized in Table 3, and it was taken from the ISO 286-1 standard.

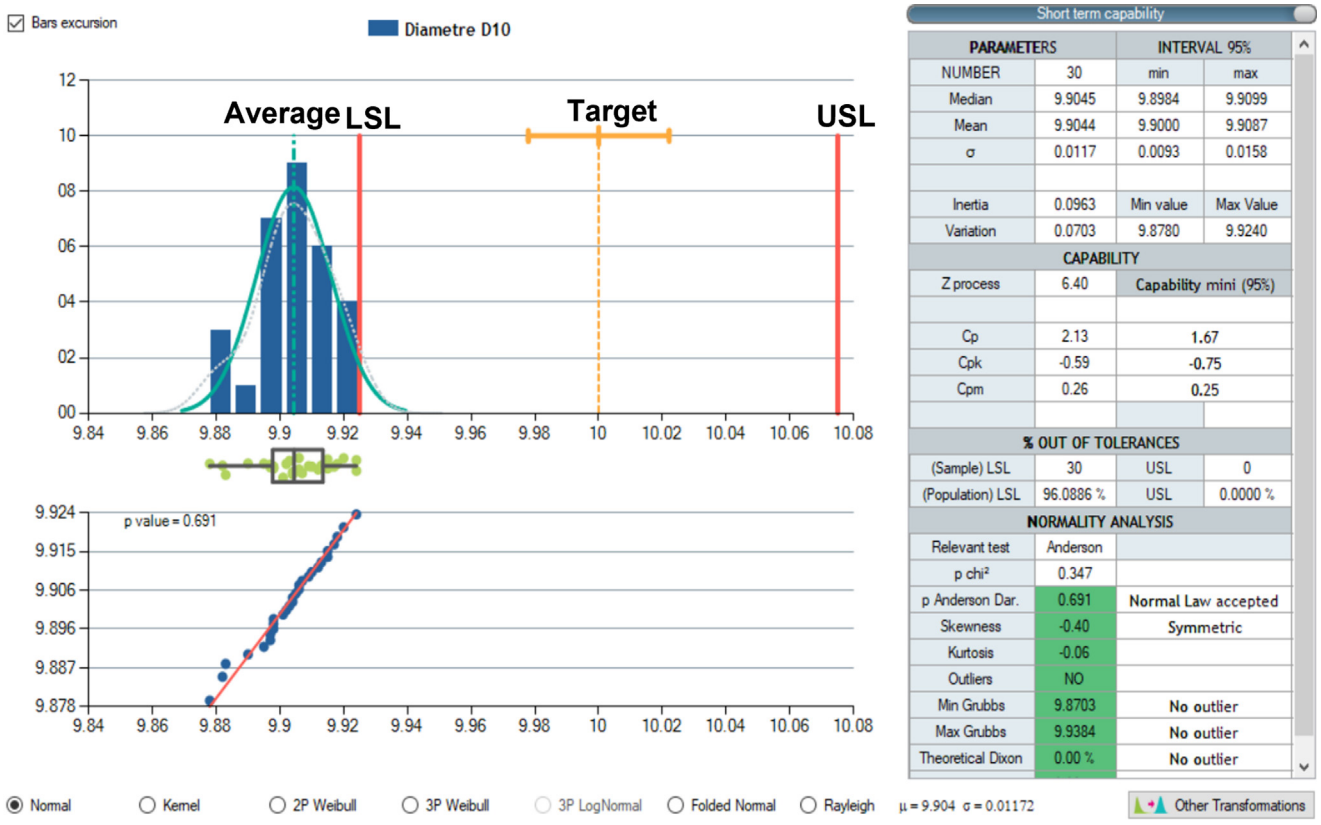

Fig. 5. Distribution of values around the mean as a histogram, the target and positioning with respect to the specified limits: the case of IT 12 for diameter D10 (Onyx parts).

All the statistical analyses of the dimensions demonstrated a normal distribution (as shown in Fig. 5). The value of Cp was found to be 1.60 for the IT12 class for the **C25** dimension, which indicates that the process is intrinsically capable and has good repeatability of the dimensions. A significant portion of the manufactured dimensions is within the specified limits, meaning that the produced parts' dimensions are within the specified tolerance. However, it should be noted that the dimensions are off-centered toward the upper boundary, resulting in a low value of Cpk (0.85). Previous studies by Günay et al. [14] reported a $Cp > 2$ in the IT12 class, which is higher than the Cp value obtained in this study. Meanwhile, other studies by Maurya et al. [6] and Maurya et al. [29] found that printed dimensions were smaller than the CAD dimensions due to material shrinkage. In contrast, the present study shows that the printed dimensions (**C25** and **C30**) are larger than the CAD dimensions due to material expansion during cooling. For the D10 diameter case with IT12 class, the Cp value was found to be approximately 2.08, indicating that the process is capable of producing repeatable hole dimensions. However, the Cpk value was less than zero, indicating a strongly off-center process. This could be attributed to material shrinkage and the servo system that drives the print heads, which generates this defect. The printed diameter was found to be smaller than the design diameter, which is consistent with the findings of previous studies by Mora et al. [30] and Rathor et al. [23].

3.2 Results for geometric features

The present study investigated the geometric features of parallelism, perpendicularity, cylindricity, and flatness. We examined the perpendicularity between surfaces **B** and **C**, the parallelism between surfaces **10** and **C**, the flatness of surfaces **A**, **B**, and **C**, and the cylindricity of hole **D10** based on the design part. To determine the general tolerance of each feature according to the standard, we calculated the IT and set a value of $Cp = 1.33$ in a bandwidth of 6σ based on the QS9000 standard [31]. Table 4 summarizes the mean deviations and tolerance intervals for the geometric features.

The tolerances obtained in this study were smaller than those obtained by Mora et al. [30], where the features deviated from 0.05 to 1.4 millimeters. This shows that the X7 printer used in this study is more efficient than the non-industrial printer used by Mora. The calculated tolerance intervals allow a classification according to the ISO 2768 standard. This classification shows class H (fine class) for the majority of geometric features.

3.3 Influence of humidity and fiber reinforcement

When polyamide material is exposed to long-term aging, it can absorb humidity from the surrounding environment. For injected plastic parts, this can cause changes in their dimensions and geometric features. The effect of moisture

Table 4. Deviations and tolerance of geometric features (Onyx parts).

Features	Mean deviation (mm)	Dispersion 6σ (mm)	Calculated IT (mm)	Class
Flatness A	0.038	0.048	0.064	H
Flatness B	0.022	0.024	0.032	H
Flatness C	0.031	0.048	0.064	H
Cylindricity D10	0.07	0.072	0.096	H
Parallelism 10/C	0.082	0.21	0.279	K
Perpendicularity B/C	0.026	0.066	0.089	H

Table 5. Moisture's Influence on calculated IT (Onyx Parts).

	Non-aged IT	Aged IT	Degradation (%)	Effect of moisture
Flatness A	0.064	0.155	+ 142.18	+++
Flatness B	0.036	0.058	+ 61.11	++
Flatness C	0.067	0.112	+ 67.16	++
Perpendicularity B/C	0.089	0.121	+ 35.95	+
Parallelism 10/C	0.282	0.387	+ 37.23	+
Cylindricity	0.096	0.116	+ 20.83	+

Table 6. Influence of reinforcing and moisture on calculated IT (reinforced parts).

	Non-aged IT	Aged IT	Degradation (%)	Effect of fibers
Flatness A	0.067	0.056	−16.41	−
Flatness B	0.321	0.23	−28.34	−
Flatness C	0.783	0.45	−42.52	−
Perpendicularity B/C	0.384	0.289	−24.73	−
Parallelism 10/C	0.742	0.45	−39.35	−
Cylindricity	0.318	0.36	+ 13.20	+

absorption is presented in Table 5, where we compared the calculated IT (ensuring a Cp of 1.33) between aged and unaged parts. Analysis of the shape deviation, specifically flatness deviation, showed a widening of the tolerance intervals and degradation of the part's shape (with an increase in IT of about 142%, 61%, and 67% respectively for the flatness deviation of surfaces **A**, **B**, and **C**). The IT of the hole cylindricity also degraded by about 21%. The deviations of parallelism and perpendicularity also experienced degradation, which is likely due to the swelling of the part when it absorbs moisture.

We also evaluated the impact of glass fiber reinforcement and aging simultaneously and summarized the results in Table 6. The findings showed a reduction in the flatness, perpendicularity, and parallelism tolerance of the reinforced parts as they aged. This improvement was likely due to the stabilization of the surfaces resulting from the glass fibers, which reduced the absorption of moisture.

A comparison of parts without and with fibers showed that the addition of fibers caused a degradation of the parts' geometric and dimensional features. This is undoubtedly due to the high rigidity of glass fibers, which means that during printing, the fibers are not straight. In fact, at the end of the printing process, the glass fibers are already not straight, as shown in Figure 6, where waviness can be observed on the glass fibers. The degradation of dimensional and geometric defects in glass fiber-reinforced parts is intrinsically due to the printer process.

For instance, the average flatness of surface **C** in parts without fibers increased by about 75% compared to reinforced parts, while the parallelism of the **10**/**C** surface degraded by up to 63%.

When comparing the IT of the **D10** diameter, we observed that the addition of fibers did not significantly improve the cylindricity deviation under the effect of aging. The increase in cylindricity deviation between aged non-reinforced and aged reinforced parts was 17% and 11%, respectively. For parts without aged reinforcements, there was a 58% increase in the flatness deviation of surface A, but a 17% decrease was observed for the reinforced parts (as shown in Fig. 7). The parts without reinforcements tended to swell under the effect of humidity, which explained the degradation of the features. However, the addition of fibers slowed down and stabilized the

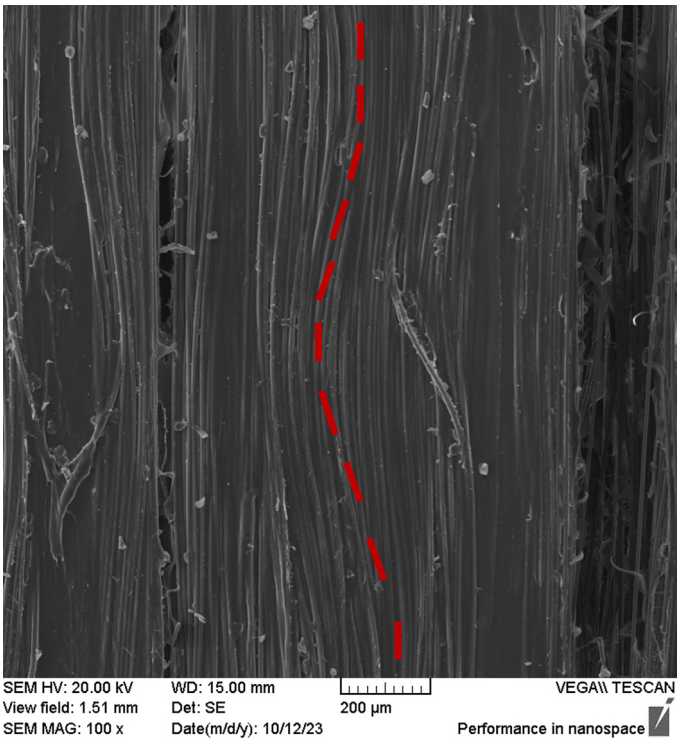

Fig. 6. Waviness of printed glass fibers.

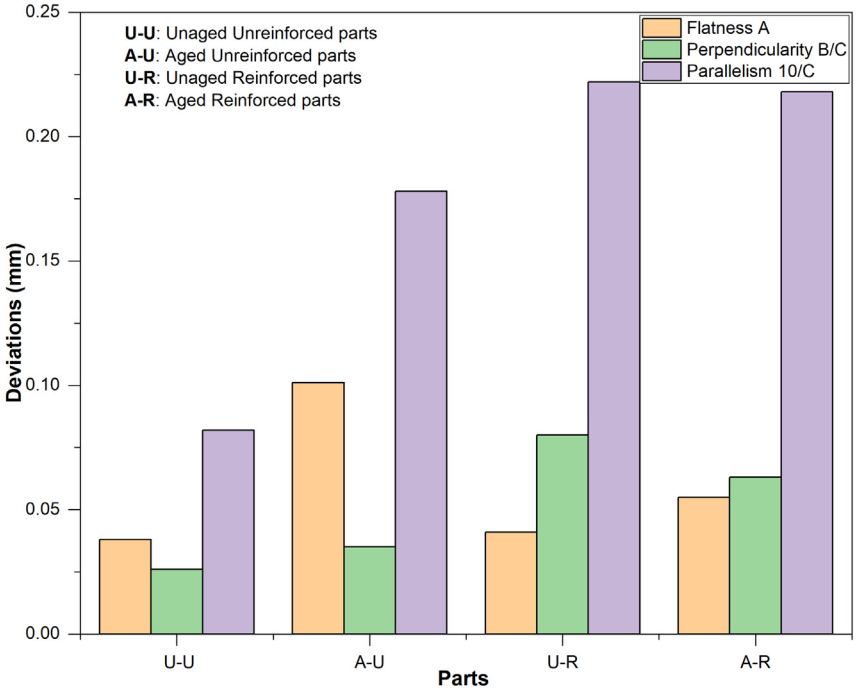

Fig. 7. Flatness deviation of surface A: a comparison of influence of moisture and fibers reinforcement.

degradation of the flatness deviations. The same observations are made for perpendicularity and parallelism (as shown in Fig. 7). It is important to consider that in order to define the tolerance intervals of parts printed with the X7 printer, it is necessary to take into account the effect of aging and fibers.

3.4 Comparison to other processes

Previous research on additive manufacturing using FDM, including the work of Lieneke et al. [5], has demonstrated that the FDM process can achieve IT levels ranging from class 9 to 14, as proposed in the ISO 286-1 standard. These

Table 7. Overview of IT by process [5].

Process	IT grade										
	7	8	9	10	11	12	13	14	15	16	17
Casting											
Sintering											
Drop forging											
Milling											
Cutting											
Turning											
Drilling											
X7 Printer											
FDM [5]											

findings were based on comparisons with other manufacturing processes, such as sintering, milling, cutting, and drilling. In a separate study, Günay et al. [14] determined that the FDM process is capable of achieving IT11 and can produce 0.19% non-conformity. In comparison, our study suggests that the FDM process is capable of achieving IT12 for linear dimensions (direct dimensions), which is comparable to forging, casting, cutting, or drilling processes. It should be noted that the dimensions produced may not precisely match the fixed IT and may vary slightly around an average, introducing the concept of process fidelity. Table 7 provides a summary of IT classes for various manufacturing processes.

4 Conclusion and perspectives

The primary aim of this study was to assess the potential of Markfoged X7 printer for industrial use, by exploring quality indices taken from the QS900 standard, specifically Cp and Cpk capability indices. The findings can be summarized as follows:

– The printer shows good performance in terms of the Cp index for IT12 tolerance intervals, with Cp ranging from 1.65 to 2 across all dimensions studied, indicating good dimension repeatability. However, the Cpk index shows that the process is not centered on the target dimensions.

– The printer generates geometric feature deviations ranging from 0.004 mm to 0.035 mm for parallelism, perpendicularity, cylindricity, and flatness. The tolerances calculated based on a Cp of 1.33 for these geometric defects range from 0.032 mm to 0.279 mm.

– The study also revealed that moisture strongly influences geometric features, resulting in an increase in defects and a wider tolerance interval. However, adding fibers stabilizes these defects over time.

– A degradation of geometric and dimensional defects, which is intrinsic to the X7 printer process, was observed between reinforced and non-reinforced parts.

– The consideration of humidity and the addition of fibers or not is then essential in the definition of tolerance intervals.

Overall, this study sheds light on the industrial potential of this printer by examining its dimensional and geometric characteristics. Future research will focus on analyzing the surface roughness of printed parts, optimizing the printing process, and capability investigation of the assembly of parts produced by this printer.

Funding

This study was not funded by any funding source or organization.

Conflict of interest

The authors declare that they have no known competing financial interests or personal relationships that could have influenced the work reported in this paper.

Ethical approval

This article does not contain any studies with human participants or animals performed by any of the authors.

CRediT authorship contribution statement

Daouda Nikiema: Conceptualization, Experimental and statistical analysis, Methodology, Validation, Writing; **Pascale Balland**: Project administration, Resources, Methodology, Supervision, Validation, Review; **Alain Sergent**: Methodology, CAD design, CMM programming, Supervision, Validation, Review.

References

[1] A. Thompson, D. McNally, I. Maskery, R.K. Leach, X-ray computed tomography and additive manufacturing in medicine: A review, Int. J. Metrol. Qual. Eng. **8**, (2017)

[2] R. Surya Teja, M. Lokesh, S. Deepak Kumar, P.S.V. Ramana Rao, 3D Printing of complex structures: case study of Eiffel Tower, Mater. Today Proc. **76**, 640–646 (2023)

[3] T. Siripongpreda, V.P. Hoven, B. Narupai, N. Rodthongku, Emerging 3D printing based on polymers and nanomaterial additives: enhancement of properties and potential applications, Eur. Polym. J. **184**, 111806 (2023)
[4] K. Kandananond, Surface roughness prediction of FFF-fabricated workpieces by artificial neural network and Box-Behnken method, Int. J. Metrol. Qual. Eng. **12**, (2021)
[5] T. Lieneke, V. Denzer, G.A.O. Adam, D. Zimmer, Dimensional tolerances for additive manufacturing: experimental investigation for fused deposition modeling, Procedia CIRP. **43**, 286–291 (2016)
[6] N.K. Maurya, V. Rastogi, P. Singh, Investigation of dimensional accuracy and international tolerance grades of 3D printed polycarbonate parts, Mater. Today Proc. **25**, 537–543 (2019)
[7] P. Minetola, F. Calignano, M. Galati, Comparing geometric tolerance capabilities of additive manufacturing systems for polymers, Addit. Manuf. **32**, 1–10 (2020)
[8] L.M. Galantucci, I. Bodi, J. Kacani, F. Lavecchia, Analysis of dimensional performance for a 3D open-source printer based on fused deposition modeling technique, Procedia CIRP. **28**, 82–87 (2015)
[9] S. Maurya, B. Malik, P. Sharma, A. Singh, R. Chalisgaonkar, Investigation of different parameters of cube printed using PLA by FDM 3D printer, Mater. Today Proc. **61**, 1217–1222 (2022)
[10] V.B. Nidagundi, R. Keshavamurthy, C.P.S. Prakash, Studies on parametric optimization for fused deposition modelling process, Mater. Today Proc. **2**, 1691–1699 (2015)
[11] C.W. Wu, W.L. Pearn, S. Kotz, An overview of theory and practice on process capability indices for quality assurance, Int. J. Prod. Econ. **117**, 338–359 (2009)
[12] M.Z. Anis, M. Tahir, On some subtle misconceptions about process capability indices, Int. J. Adv. Manuf. Technol. **87**, 3019–3029 (2016)
[13] R. Mahshid, Z. Mansourvar, H.N. Hansen, Tolerance analysis in manufacturing using process capability ratio with measurement uncertainty, Precis. Eng. **52**, 201–210 (2018)
[14] E.E. Günay, A. Velineni, K. Park, G.E. Okudan Kremer, An Investigation on Process Capability Analysis for Fused Filament Fabrication, Int. J. Precis. Eng. Manuf. **21**, 759–774 (2020)
[15] N. Ranjan, Materials today: proceedings process capability analysis for fabrication of high elongated PVC polymer using extrusion process selection of thermoplastic polymer (PVC) average feedstock filament has been calculated for reducing of measurement error sel, J. Mater. Today: Proc. **48**, 1731–1734 (2022)
[16] Y. Wooluru, D.R. Swamy, P. Nagesh, The process capability analysis - a tool for process performance measures and metrics - a case study, Int. J. Qual. Res. **8**, 399–416 (2014)
[17] M. Aclan, R. Oezden, S. Danho, Investigation of the geometric change of plastic articles made by polyamide, in: MATEC Web Conf., EDP Sciences, 2018
[18] I. Clavería, D. Elduque, J. Santolaria, C. Pina, C. Javierre, A. Fernandez, The influence of environmental conditions on the dimensional stability of components injected with PA6 and PA66, Polym. Test. **50**, 15–25 (2016)
[19] Markforged, X7 Gen2, (2021) 1. https://s3.amazonaws.com/mf.product.doc.images/Datasheets/F-PR-3012.pdf. (accessed October 16, 2021)
[20] A. Vlaicu, L.I. Repanovici, Acta technica napocensis, Acta Tech. Napocensis. **64**, 207–210 (2021)
[21] D.R. Hetrick, S.H.R. Sanei, C.E. Bakis, O. Ashour, Evaluating the effect of variable fiber content on mechanical properties of additively manufactured continuous carbon fiber composites, J. Reinf. Plast. Compos. **40**, 365–377 (2021)
[22] D. Nikiema, P. Balland, A. Sergent, Study of the mechanical properties of 3D-printed onyx parts: investigation on printing parameters and effect of humidity, Chinese J. Mech. Eng. Addit. Manuf. Front. **2**, 100075 (2023)
[23] S. Singh Rathor, A. Sharma, Y.K. Modi, PROCESS Capability Analysis of Fused Deposition Modeling Process, Int. j. adv. eng. technol. 11, 147–154 (2018)
[24] ELLISTAT, (n.d.). https://ellistat.com/. (accessed March 18, 2023)
[25] S. Khodaygan, M.R. Movahhedy, Functional process capability analysis in mechanical systems, Int. J. Adv. Manuf. Technol. **73**, 899–912 (2014)
[26] J. Rajashekharaiah, Six sigma benchmarking of process capability analysis and mapping of process parameters, J. Oper. Supply Chain Manag. **9**, 60 (2017)
[27] DIN EN ISO 286-1:2010, Geometrical product specifications (GPS) — ISO code system for tolerances on linear sizes — Part 1: Basis of tolerances, deviations and fits, Iso. 2010 (2010)
[28] P.R. Gradl, D.C. Tinker, J. Ivester, S.W. Skinner, T. Teasley, J.L. Bili, Geometric feature reproducibility for laser powder bed fusion (L-PBF) additive manufacturing with Inconel 718, Addit. Manuf. **47**, (2021)
[29] S. Maurya, B. Malik, P. Sharma, A. Singh, R. Chalisgaonkar, Investigation of different parameters of cube printed using PLA by FDM 3D printer, Mater. Today Proc. **64**, 1217–1222 (2022)
[30] S.M. Mora, J.C. Gil, A.M.C. López, Influence of manufacturing parameters in the dimensional characteristics of ABS parts obtained by FDM using reverse engineering techniques, Procedia Manuf. **41**, 968–975 (2019)
[31] D.H. Stamatis, Quality System Requirements, 2019. https://doi.org/10.4324/9780203734742-3.

Cite this article as: D. Nikiema, A. Sergent, P. Balland, Study of the industrial potential of Markforged X7 3D printer, Mechanics & Industry **25**, 4 (2024)